Supporting Information

Hybrid tantalum oxide nanoparticles from the hydrolysis of imidazolium tantalate ionic liquids: efficient catalysts for hydrogen generation from ethanol/water solutions

Virgínia S. Souza,[a] Jackson D. Scholten,*[a] Daniel E. Weibel,[a] Dario Eberhardt,[b,c] Daniel L. Baptista,[c] Sérgio R. Teixeira[c] and Jairton Dupont*[a,d]

[a] *Instituto de Química-UFRGS, Av. Bento Gonçalves, 9500, Bairro Agronomia, CEP 91501-970, Porto Alegre-RS, Brazil.*

[b] *Universidade de Caxias do Sul, Campus Vinhedos, Alameda João Dal Sasso, 70, Bairro Universitário, Bento Gonçalves-RS, Brazil.*

[c] *Instituto de Física-UFRGS, Av. Bento Gonçalves, 9500, Bairro Agronomia, CEP 91501-970, Porto Alegre-RS, Brazil.*

[d] *School of Chemistry, University of Nottingham, University Park, Nottingham, UK, NG7 2RD.*

Corresponding authors: jackson.scholten@ufrgs.br; jairton.dupont@nottingham.ac.uk

Summary

1. Experimental section

1.1. Photocatalytic reactions

1.1.1. Quantification of the photogenerated gases

The gases formed from the photocatalytic reaction were quantified by gas chromatography (GC) using an Agilent 6820 equipped with a Porapak Q. 80/100 Mesh column and argon as carrier gas. The generated gases were simultaneously analyzed with a thermal conductivity detector (TCD) and a flame ionization detector (FID). Aliquots of 50 µL from the gas phase were removed from the reaction in intervals of 30 min and injected with a syringe containing a Hamilton sample lock valve. For calibration purposes, the standard gases H_2, CO, CO_2, CH_4, C_2H_4, and C_2H_6 were purchased from White Martins.

1.1.2. Apparent quantum yield

The apparent quantum yield of the photocatalytic reaction was calculated considering the ratio between the H_2 molecules formed and the number of absorbed photons. In order to measure the amount of photons emitted by the lamp at the wavelength of 254 nm, it was used the actinometry approach (see C. G. Hatchard and C. A. Parker, *Proc. R. Soc. A*, 1956, **235**, 518-536; S. Ahmed, *J. Photochem. Photobiol. A: Chem.*, 2004, **161**, 151-154). Initially, three identical solutions containing 3 mL of sodium acetate (1 moL/L), 3 mL of ortho-phenanthroline (0,1%), and 1 mL of ammonium fluoride (1 mol/L) were prepared in volumetric balloons of 50 mL 1, 2, and 3. All the balloons were covered with aluminum foil in order to keep the solutions in the absence of light. To the balloon 1, 10 mL of potassium ferrioxalate was added to the solution and keep without exposure to light in order to use it as a blank solution.

In another procedure, 10 mL of potassium ferrioxalate was introduced into the reactor and it was exposed to the Xe lamp allowing only the irradiation at 254 ± 10 nm (FWHM Newport filter) during 60 s in order to reduce the Fe(III) to Fe (II). After, this irradiated solution was added and mixed with the previous solution presented into balloon 2. Then, the generated Fe(II) was quantified by the formation of a complex in the presence of ortho-phenanthroline, $[Fe(phen)_3]^{2+}$. To measure the apparent quantum yield, a typical photocatalytic solution containing the tantalum oxide NPs was prepared and irradiated with the 254 nm wavelength for 45 min. For calculation purposes, it was considered that all the photons that hit the NPs' surface were absorbed. After photolysis

(45 min), the same procedure was repeated: 10 mL of potassium ferrioxalate was exposed to the Xe lamp at 254 nm during 60 s. This irradiated solution was added to the balloon 3 in order to verify if there is some variation in the emission of the photons by the lamp along the time.

At the end of these steps, it was performed the UV-Vis measurements of the solutions in balloons 1, 2, and 3. By using their absorbance, the flux of photons emitted at 254 nm can be calculated from equation 1:

$$Nh\nu\left(quanta.cm^{-3}.s^{-1}\right)=\frac{d[Fe^{2+}]/dt}{\Phi} \qquad (1)$$

where Φ means the quantum yield of the photoreduction from Fe^{3+} to Fe^{2+}, which has the value of 1.21 (Fe^{2+} molecules/quanta), and *t* is the time of irradiation. The concentration of Fe^{2+} can be determined using equation 2:

$$[Fe^{2+}]=\frac{Abs_{(510nm)}.V_1.V_2}{10^3.V_3.I.\varepsilon_{(510nm)}} \qquad (2)$$

$[Fe^{2+}]$: concentration of Fe^{2+} formed after irradiation;

$Abs_{(510nm)}$: absorbance (510 nm) of the solution irradiated for 60 s;

V_1: volume of the potassium ferrioxalate solution irradiated for 60 s (10 mL);

V_2: total volume of the actinometric solution (17 mL);

V_3: volume of the aliquot removed from the potassium ferrioxalate solution after irradiation. In this case all the solution (10 mL) has been used;

I: optic pathlength (1.0 cm);

$\varepsilon_{(510nm)}$: molar absorption coefficient of the complex $[Fe(phen)_3]^{2+}$ at 510 nm (11100 $L.mol^{-1}.cm^{-1}$).

Using equations 1 and 2 it is possible to obtain the general equation 3:

$$Nh\nu=\frac{Abs_{(510nm)}.V_1.V_2}{10^3.V_3.I.\varepsilon_{(510nm)}.\Phi.t} \qquad (3)$$

The apparent quantum yield (Φ_{app}) of the photocatalytic system was calculated from equation 4:

$$\Phi_{app} = \frac{2N_{mols}(mol.s^{-1})}{Nh\nu(quanta.cm^{-3}.s^{-1})} \qquad (4)$$

where

Φ_{app}: apparent quantum yield;

N_{mols}: number of mols of H_2 photogenerated per time unit;

Nhν: number of absorbed photons per time unit.

2. Characterization of the imidazolium tantalate ILs

Table S1. Experimental analysis of the imidazolium tantalate ILs

Sample	Infrared (cm^{-1})	Melting point (ºC)	Mass by ESI-MS (m/z)	$T_{decomposition}$ (ºC)[a]
IL **1**	816 (Ta-Cl)	63.7	392.76 ($TaCl_6^-$) 139.12 (BMI^+)	340
IL **2**	833 (Ta-Cl)	44.6	392.76 ($TaCl_6^-$) 223.22 (DMI^+)	270

[a] Initial thermal decomposition.

Table S2. ^1H and ^{13}C chemical shifts of imidazolium tantalate ILs

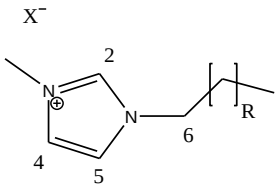

X-	R	C2 δ (ppm)	H2 δ (ppm)	C4 δ (ppm)	H4 δ (ppm)	C5 δ (ppm)	H5 δ (ppm)	C6 δ (ppm)	H6 δ (ppm)
Cl^-	2	138.0	9.74	124.1	7.53	123.0	7.49	49.5	4.22
$TaCl_6^-$	2	136.5	8.44	124.5	7.38	123.0	7.35	50.5	4.15
Cl^-	8	138.0	9.60	123	7.47	124.0	7.49	50.0	4.20
$TaCl_6^-$	8	136.4	8.43	124.4	7.38	123.0	7.35	50.4	4.13

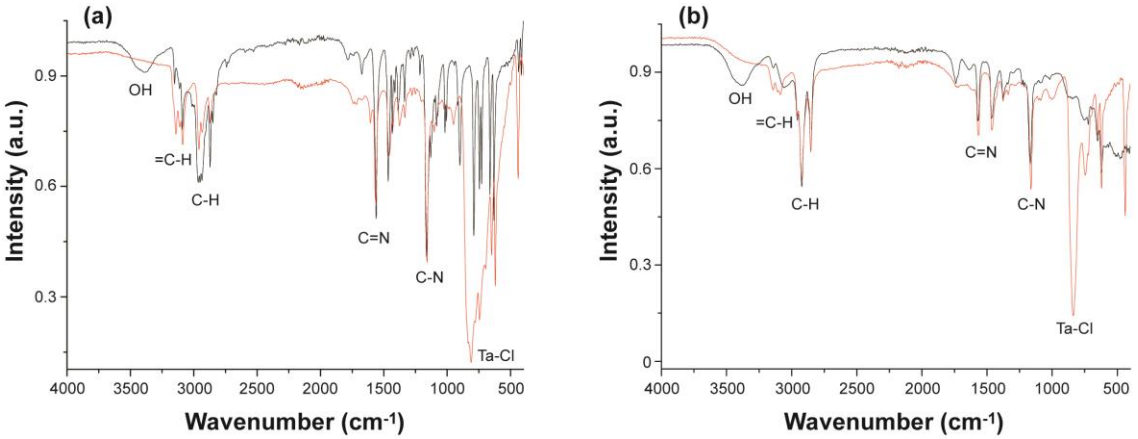

Figure S1. Infrared spectrum of ionic liquids: **(a)** BMI.Cl (black) and its respective tantalate IL **1** (red); **(b)** DMI.Cl (black) and its respective tantalate IL **2** (red).

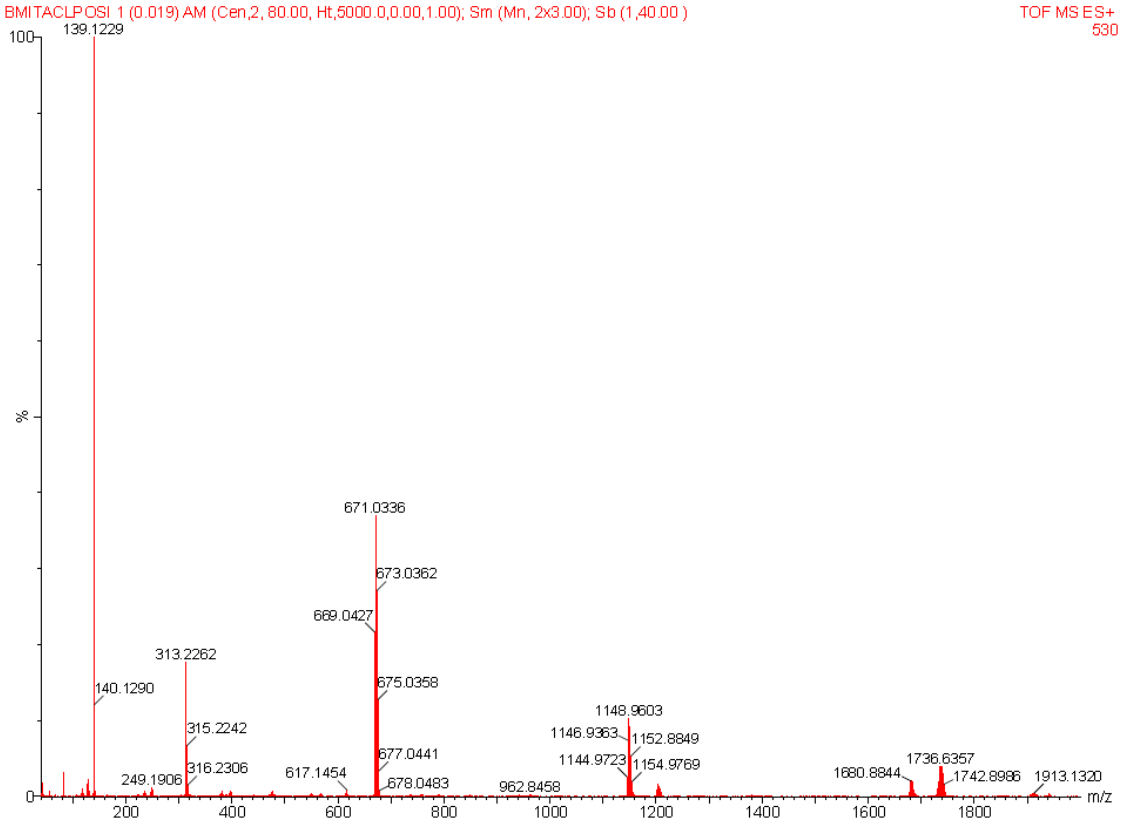

Figure S2. ESI-MS(+) spectrum of the IL **1** in acetonitrile (10^{-2} mol/L). The signal at m/z 139.1229 is related to the BMI cation (m/z calculated = 139.12 (100%)). The signals centered at m/z 671.0336, small signal around 1205 and 1736.6357 correspond to the ionic clusters $[C_2A]^+$, $[C_3A_2]^+$ and $[C_4A_3]^+$, respectively (C is the cation and A is the anion).

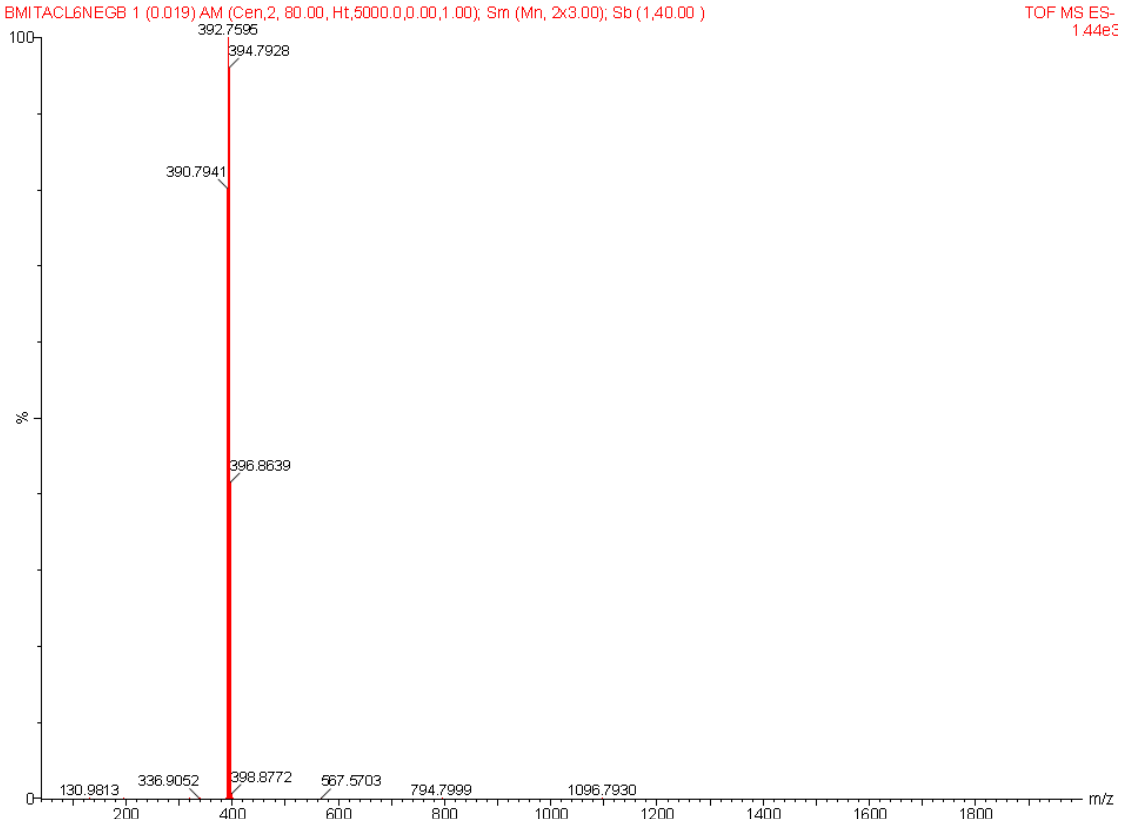

Figure S3. ESI-MS(–) spectrum of the IL **1** showing an intense signal centered at m/z 392.7595 from the anion $TaCl_6^-$ (m/z calculated = 392.76 (100%)).

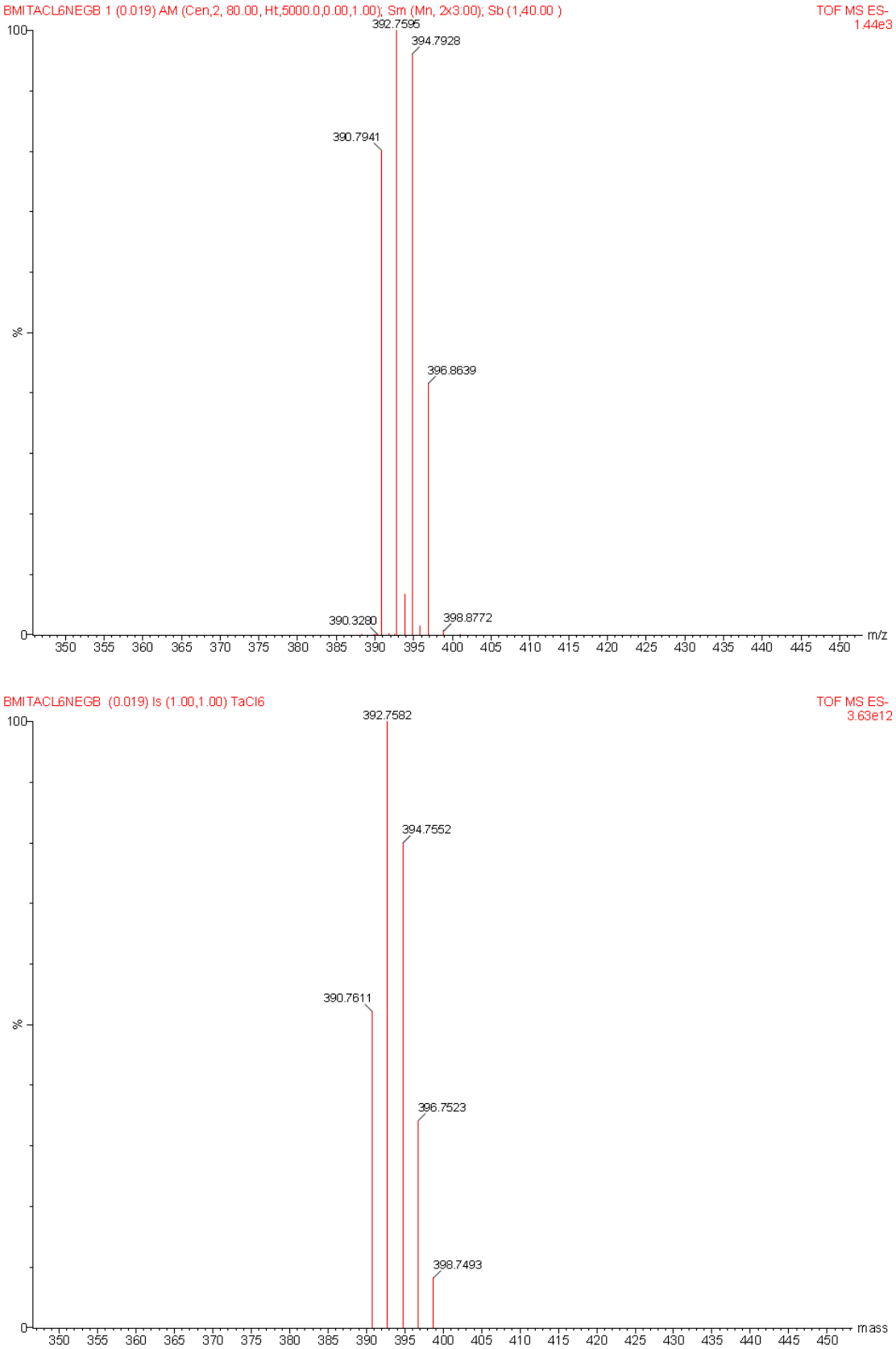

Figure S4. (top) Expanded ESI-MS(–) spectrum of IL **1** evidencing the presence of the $TaCl_6^-$ (m/z calculated = 392.76 (100%)); (bottom) simulated isotopic model spectrum.

Figure S5. ESI-MS(+) spectrum of the IL **2** in acetonitrile (10^{-2} mol/L). The signal observed at m/z 223.2181 comes from the DMI cation (m/z calculated = 223.22 (100%)). The cluster $[C_2A]^+$ was detected at m/z 839.3705 (C is the cation and A is the anion).

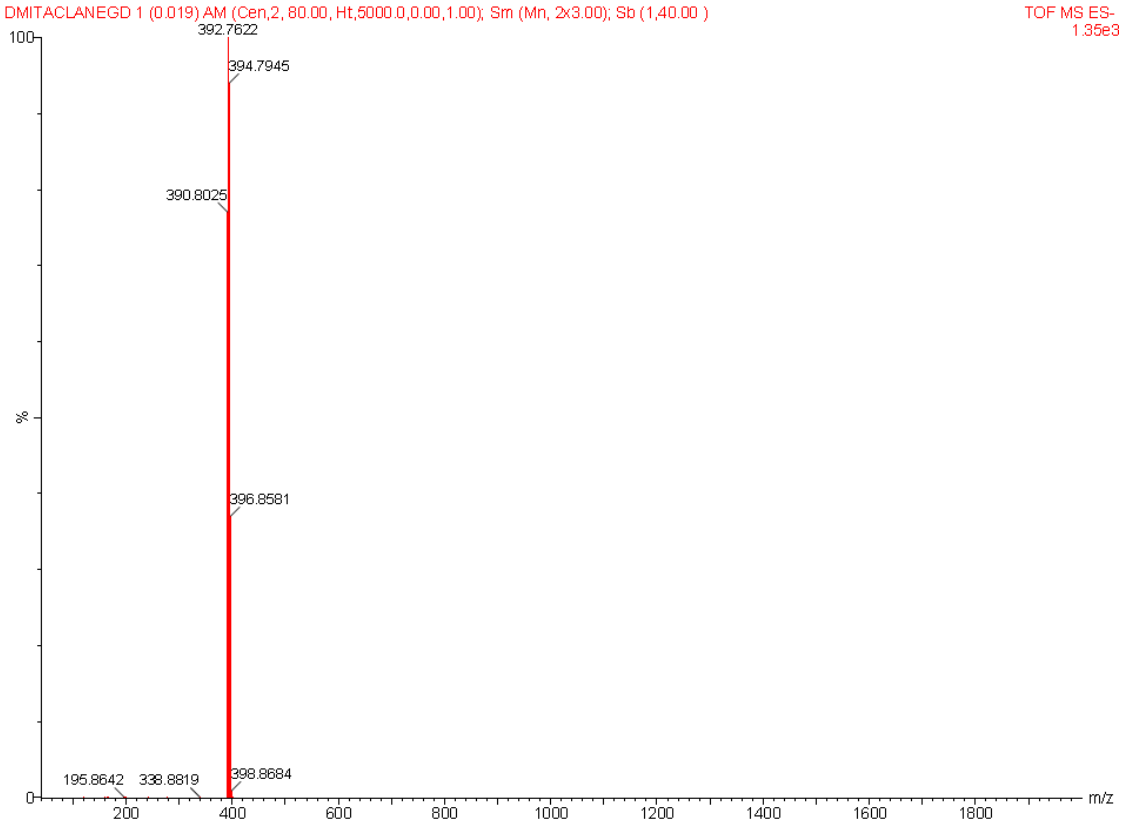

Figure S6. ESI-MS(–) spectrum of the IL **2** showing an intense signal centered at m/z 392.7622 from the anion $TaCl_6^-$ (m/z calculated = 392.76 (100%)).

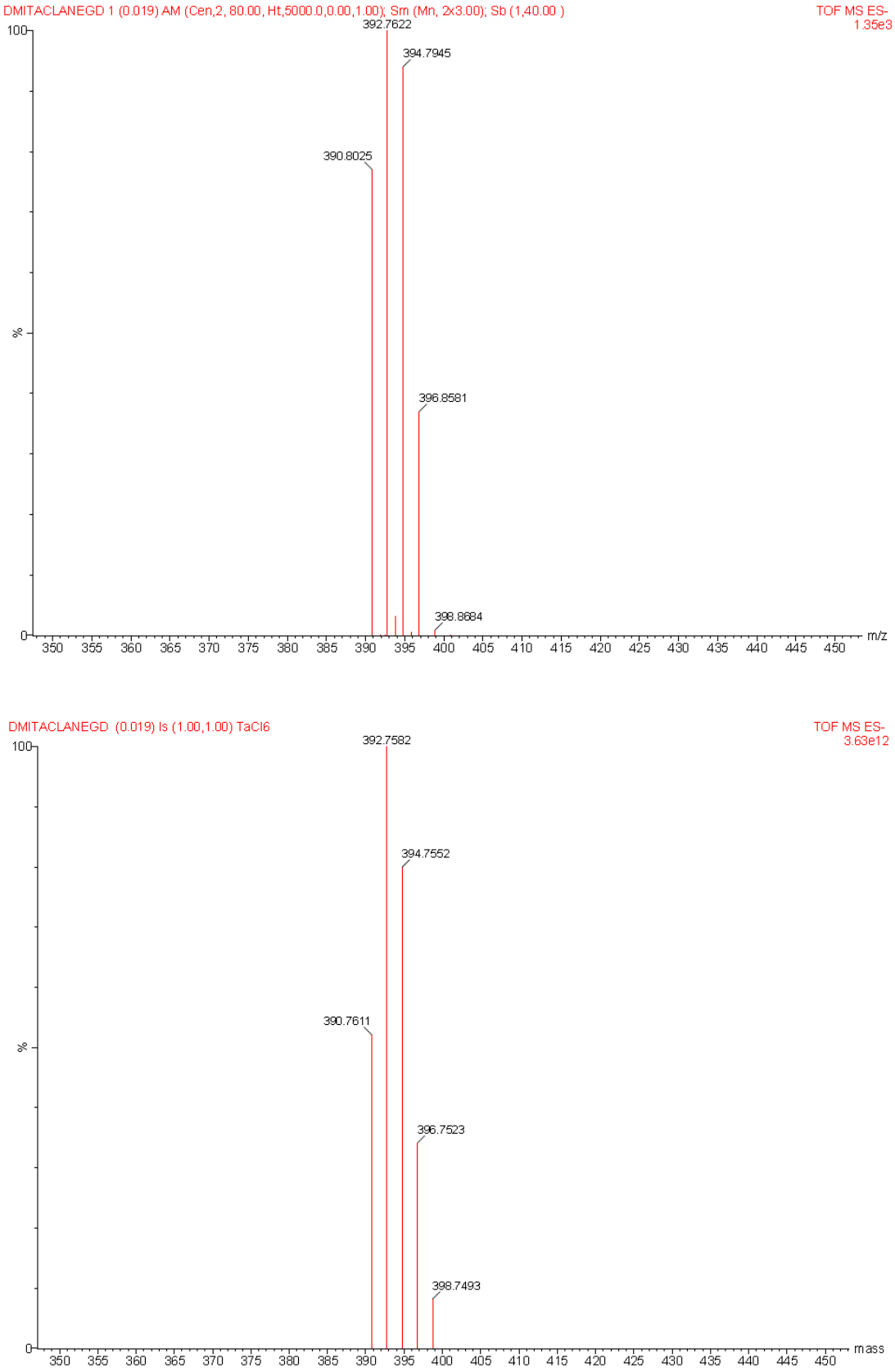

Figure S7. (top) Expanded ESI-MS(–) spectrum of IL **2** showing the signals at m/z 392.7622 (m/z calculated = 392.76 (100%)); (bottom) simulated isotopic model spectrum.

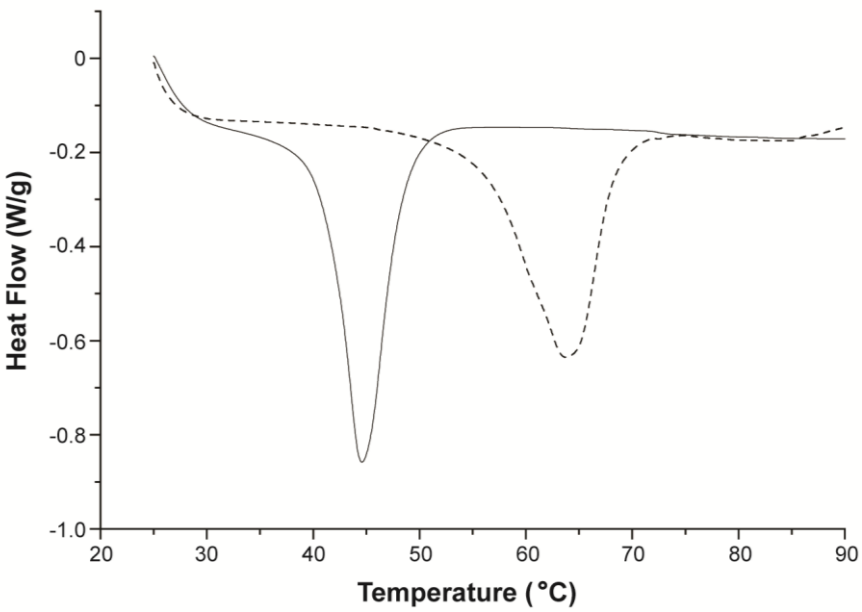

Figure S8. DSC measurements of the imidazolium tantalate ILs (expanded region): (dashed line) IL **1** and (line) IL **2**.

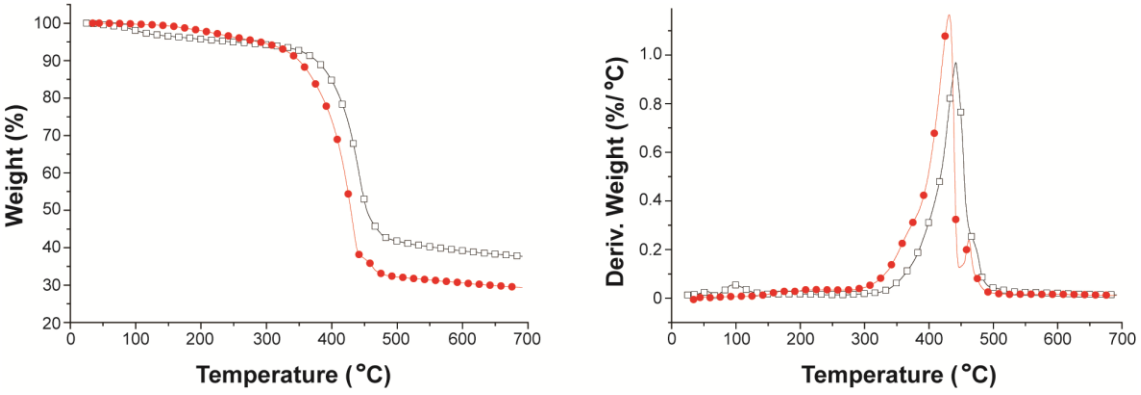

Figure S9. TGA analysis of the imidazolium tantalate ILs: (□) IL **1** and (●) IL **2**.

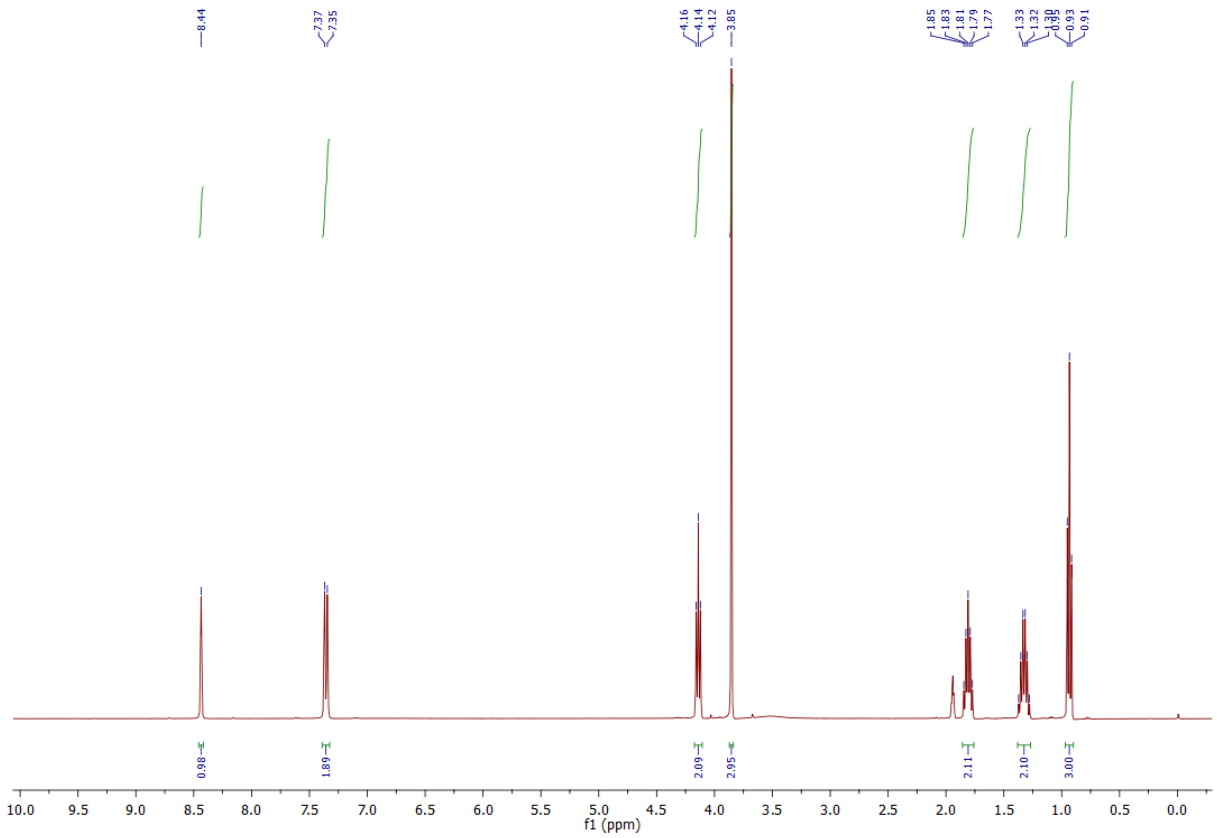

Figure S10. ^{1}H NMR (400 MHz) of the IL **1** in acetonitrile-d_3.

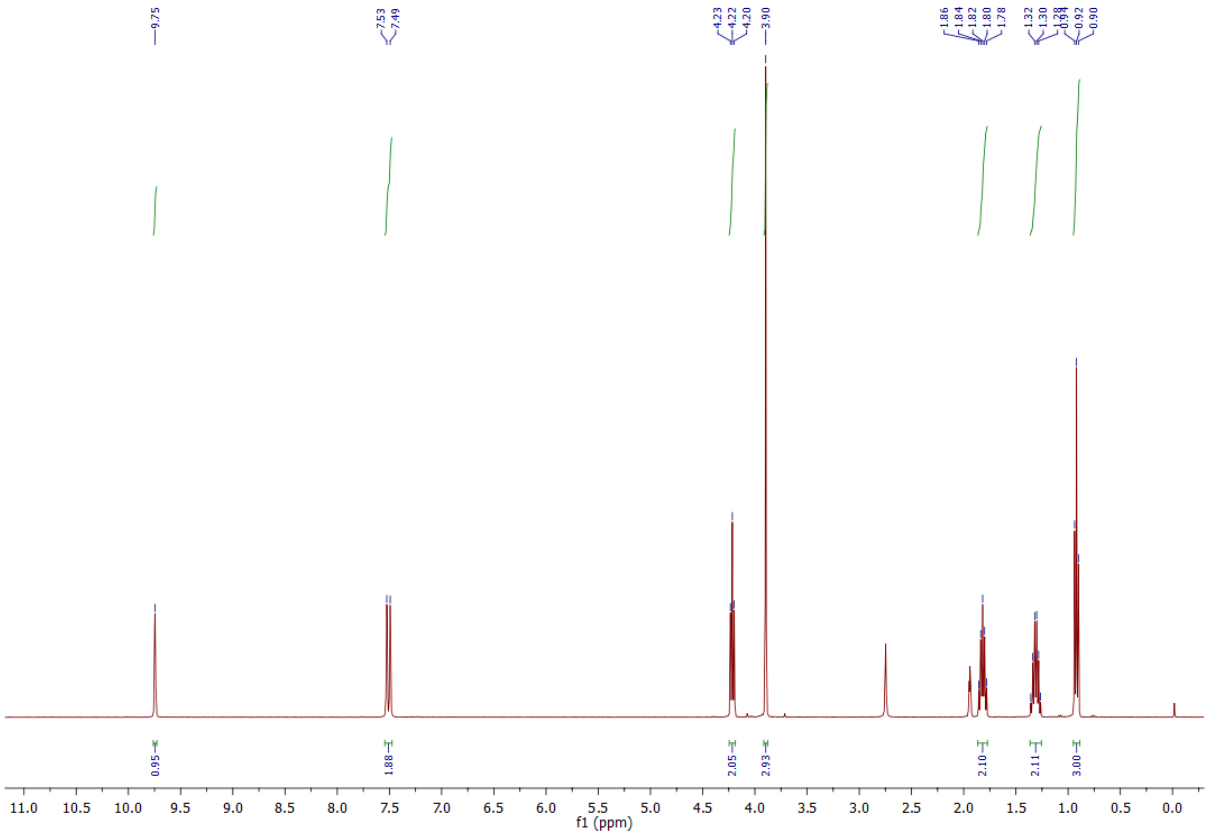

Figure S11. ^{1}H NMR (400 MHz) of the BMI.Cl IL in acetonitrile-d_3.

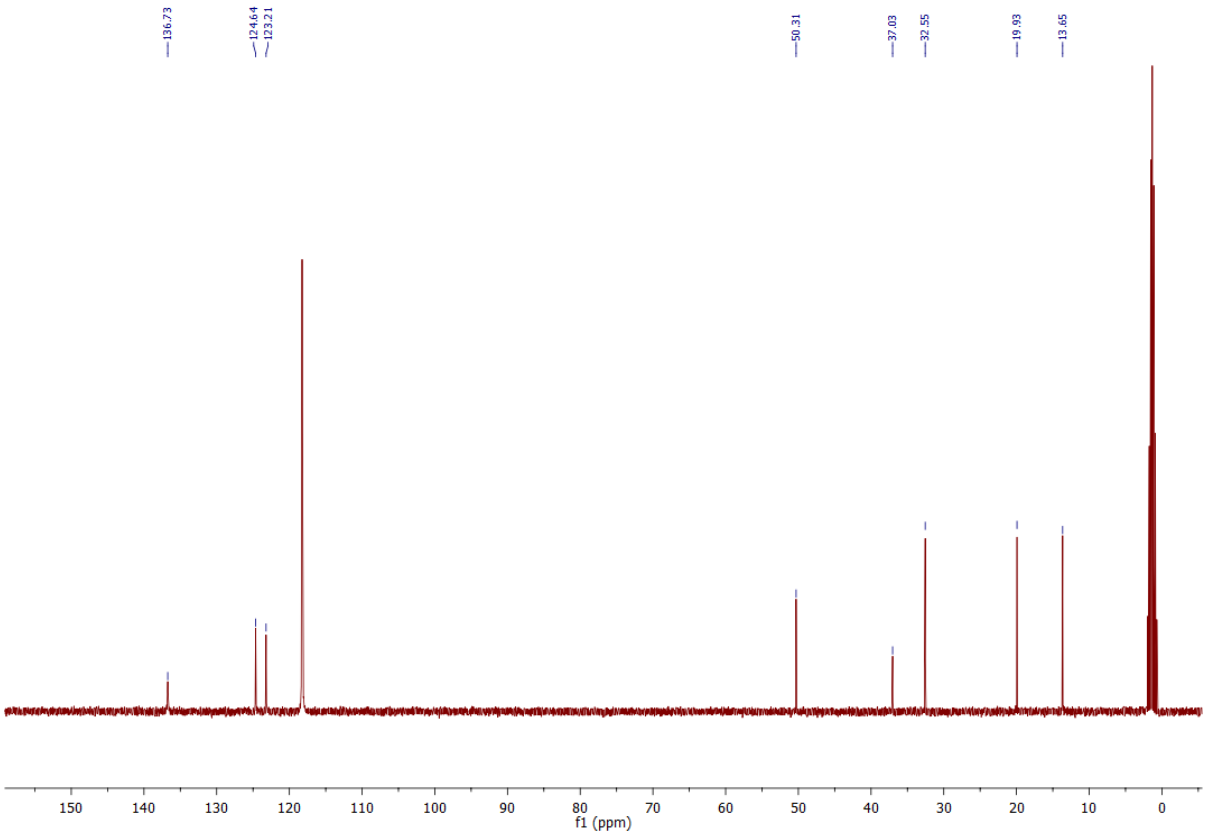

Figure S12. ^{13}C NMR-{^{1}H} (100 MHz) of the IL **1** in acetonitrile-d_3.

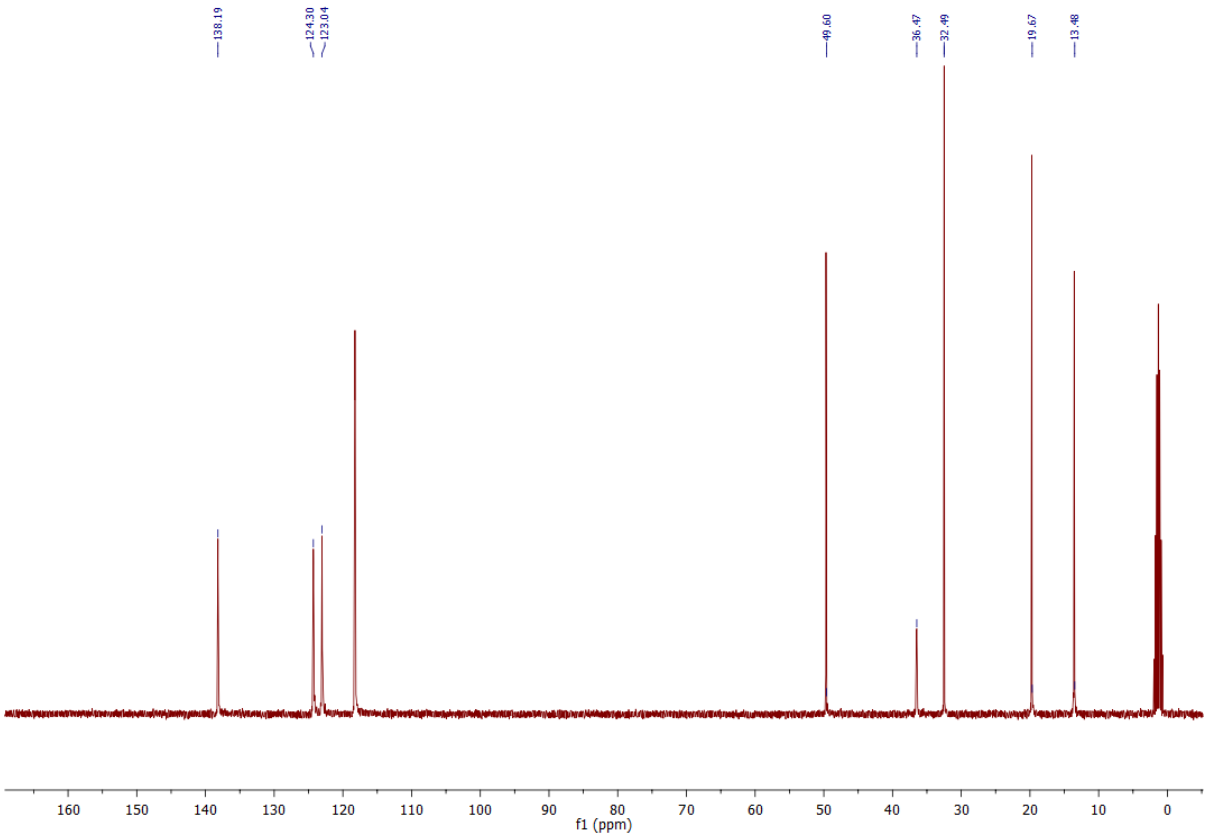

Figure S13. ^{13}C NMR-{^{1}H} (100 MHz) of the BMI.Cl IL in acetonitrile-d_3.

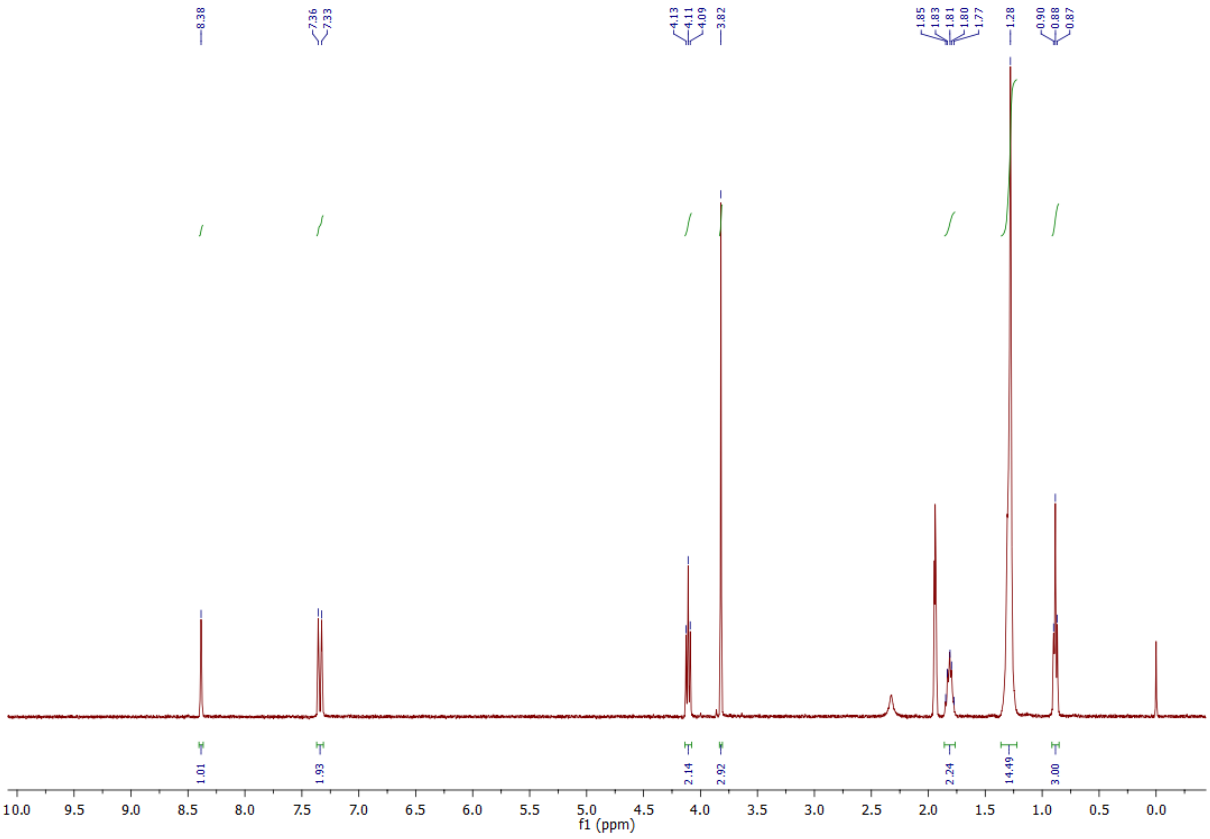

Figure S14. ^{1}H NMR (400 MHz) of the IL **2** in acetonitrile-d_3.

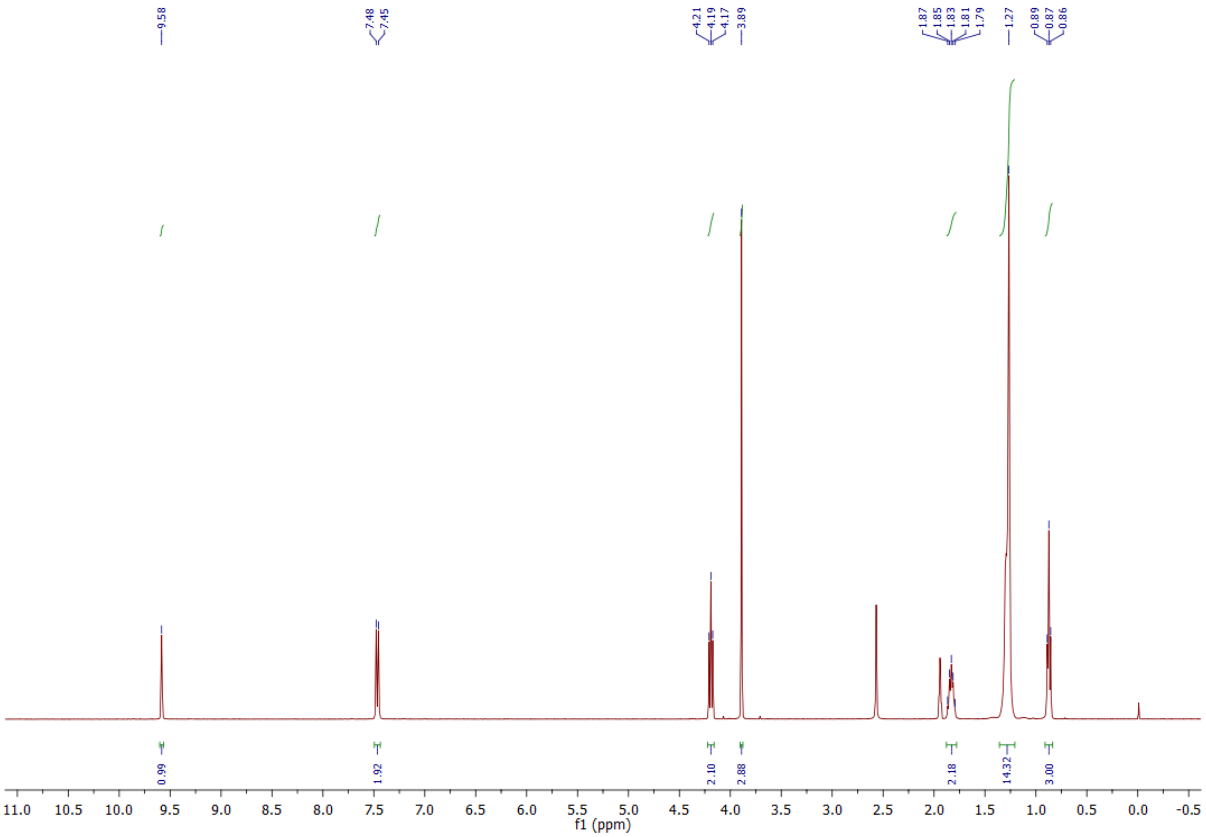

Figure S15. ^{1}H NMR (400 MHz) of the DMI.Cl IL in acetonitrile-d_3.

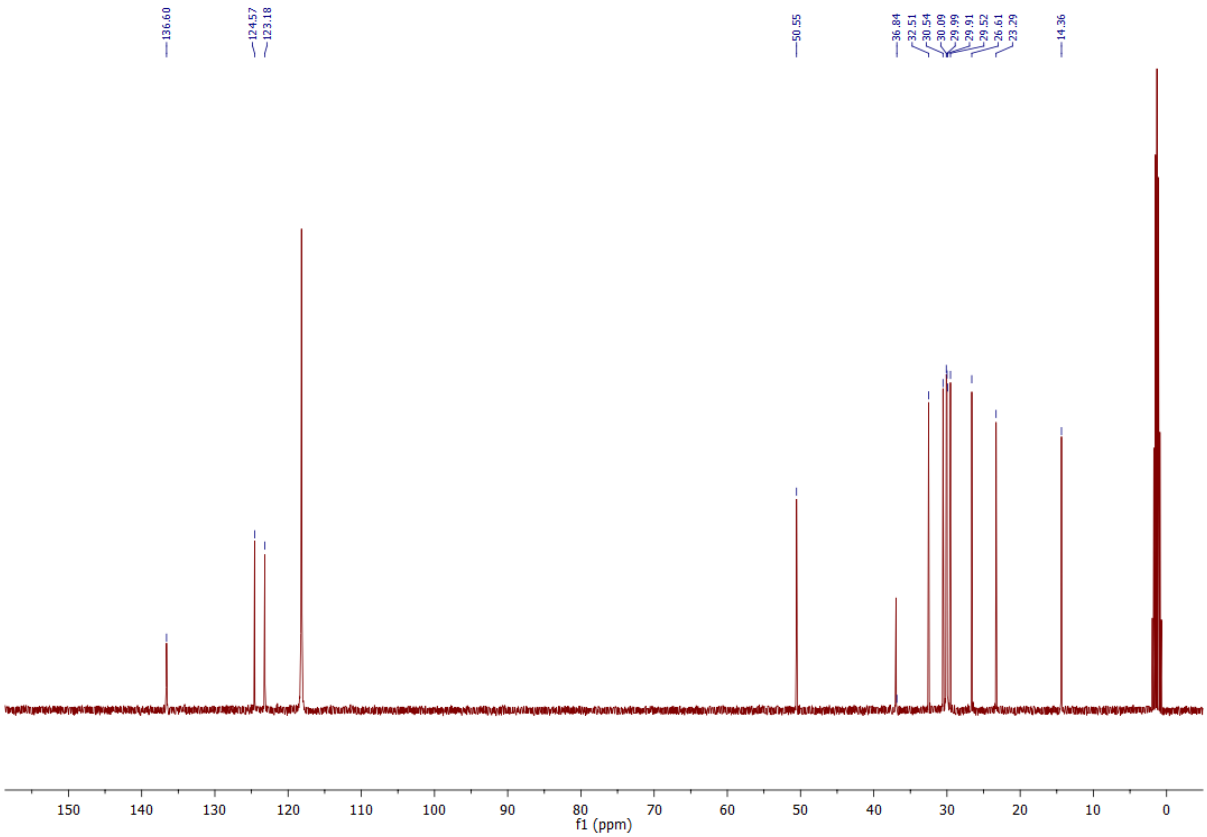

Figure S16. ^{13}C NMR-{^{1}H} (100 MHz) of the IL **2** in acetonitrile-d_3.

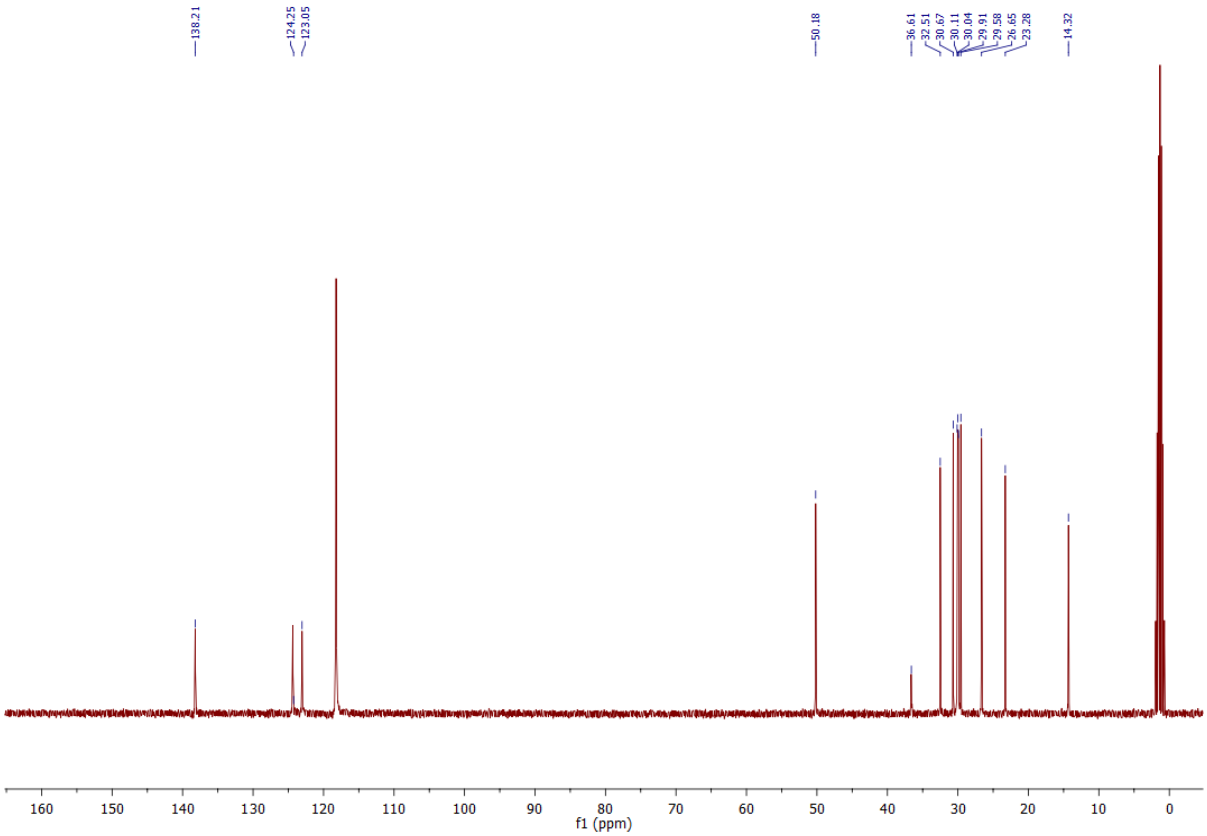

Figure S17. ^{13}C NMR-{^{1}H} (100 MHz) of the DMI.Cl IL in acetonitrile-d_3.

3. Characterization of the Ta_2O_5 NPs

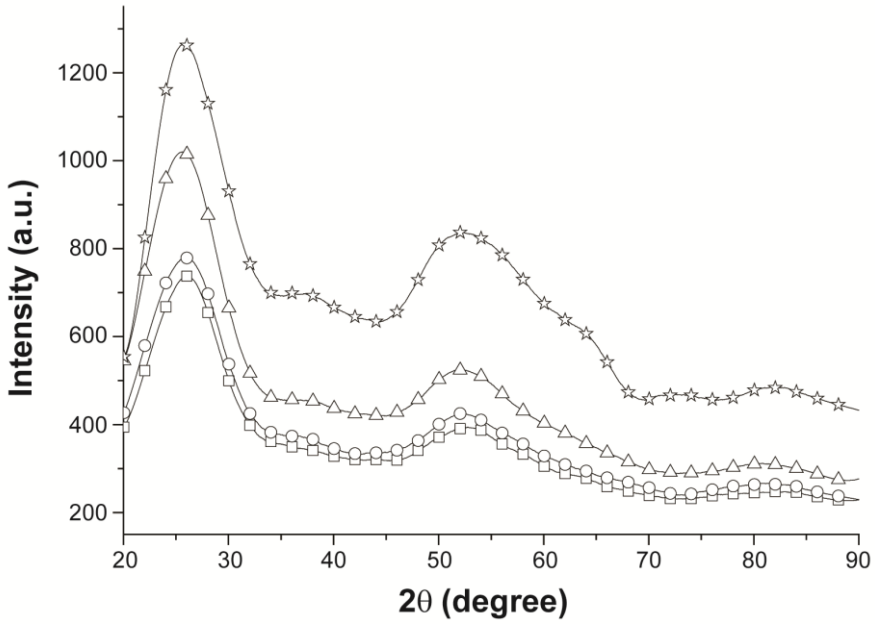

Figure S18. XRD of the as-prepared hybrid-like Ta_2O_5/IL NPs from the hydrolysis of imidazolium tantalate ILs: (☆) IL **1**/water (2:5), (Δ) IL **1**/water (2:2.5), (□) IL **2**/water (2:5) and (○) IL **2**/water (2:2.5). IL/water initial molar ratio.

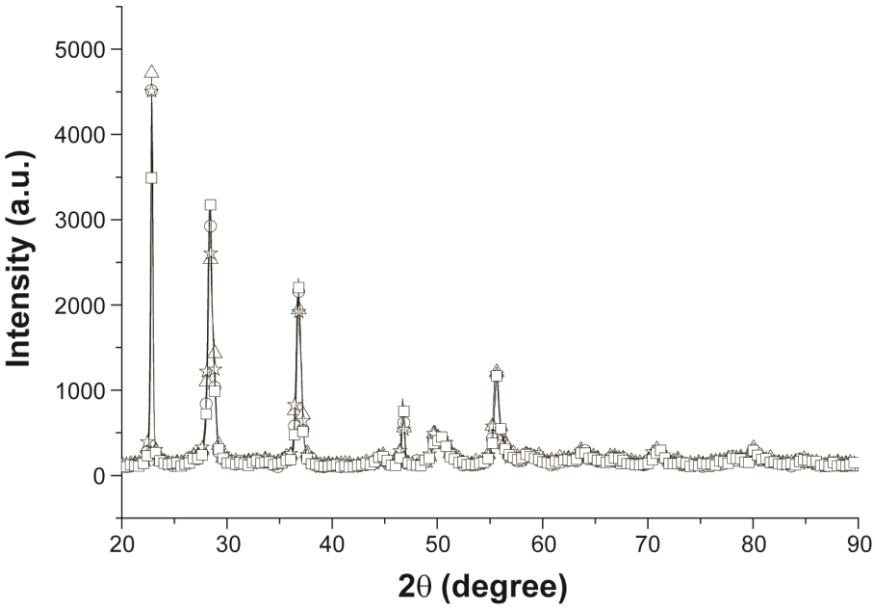

Figure S19. XRD of the Ta_2O_5 NPs after thermal treatment at 800 °C for 2 h (orthorhombic structure): (☆) IL **1**/water (2:5), (Δ) IL **1**/water (2:2.5), (□) IL **2**/water (2:5) and (○) IL **2**/water (2:2.5). IL/water initial molar ratio.

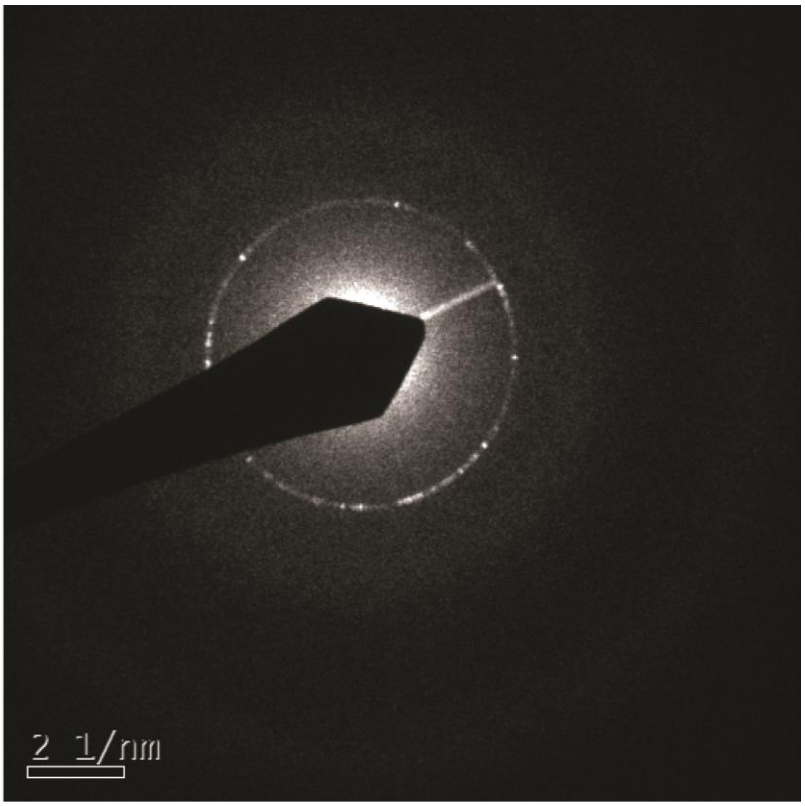

Figure S20. TEM analysis in the electron diffraction mode of the sample Ta_2O_5/IL NPs prepared from the system IL **2**/water (2:2.5, IL:water initial molar ratio). The distance d = 3.16Å corresponds to the crystalline plane (110).

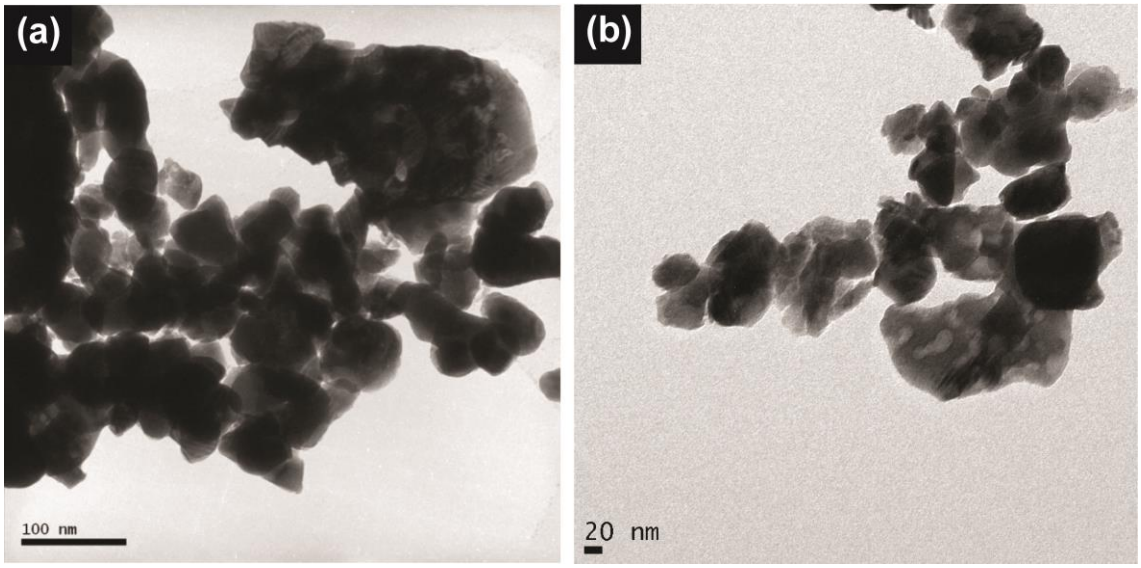

Figure S21. Typical TEM images of the Ta_2O_5 after thermal treatment at 800 °C for 2 h: **(a)** the sample was prepared from the system IL **1**/water (2:2.5, IL:water initial molar ratio); **(b)** the sample was prepared from the system IL **1**/water (2:5, IL:water initial molar ratio).

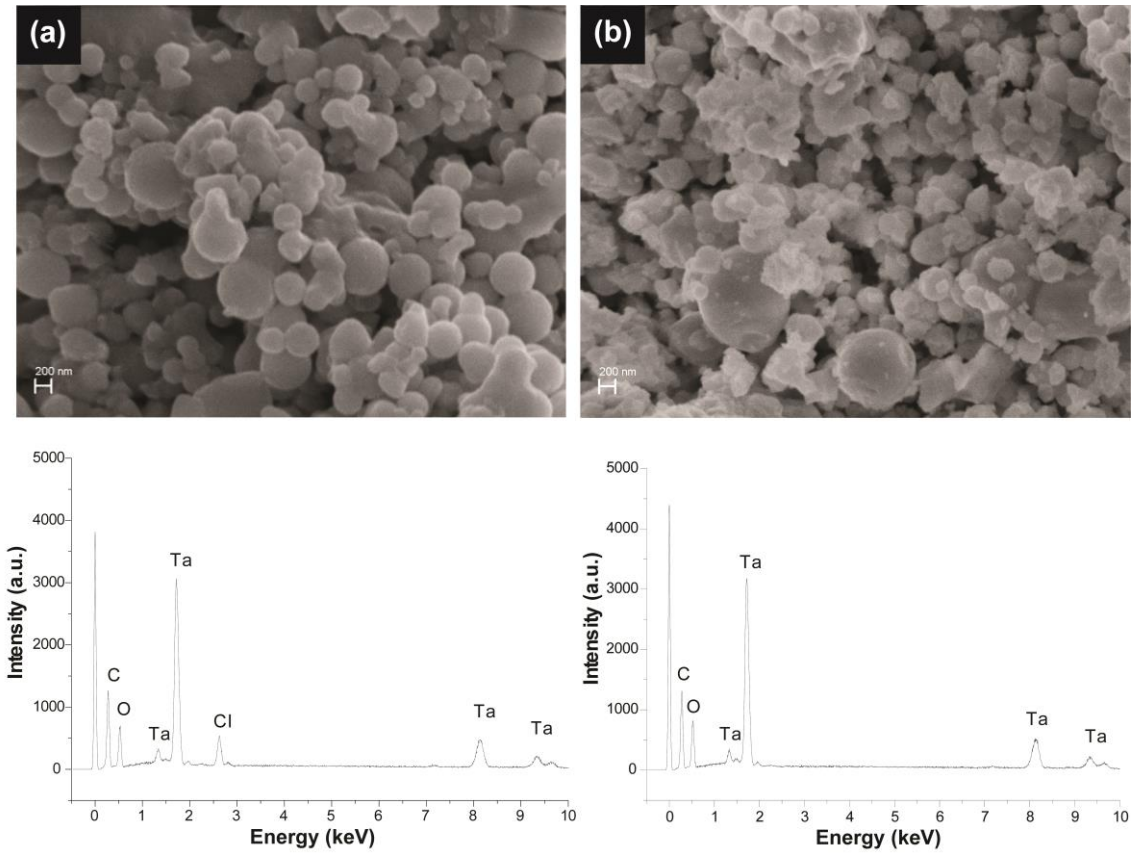

Figure S22. SEM images of Ta_2O_5 NPs prepared from IL **2**/water (2:2.5) **(a)** as-prepared (Ta_2O_5/IL); **(b)** after calcination at 800 ºC for 2 h.

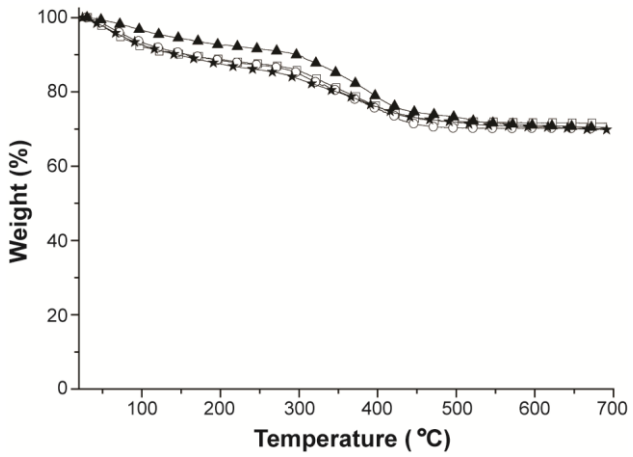

Figure S23. TGA analysis of the as-prepared Ta_2O_5/IL NPs prepared from: (□) IL **1**/water (2:5); (○) IL **1**/water (2:2.5); (▲) IL **2**/water (2:5) and (★) IL **2**/water (2:2.5). The amount of residual IL in each sample is 17.2%, 18.3%, 22.2% and 17.7%, respectively. These values were obtained considering the relative weight loss in the temperature range of 200-700 °C.

4. Characterization of the Pt-supported Ta_2O_5 NPs

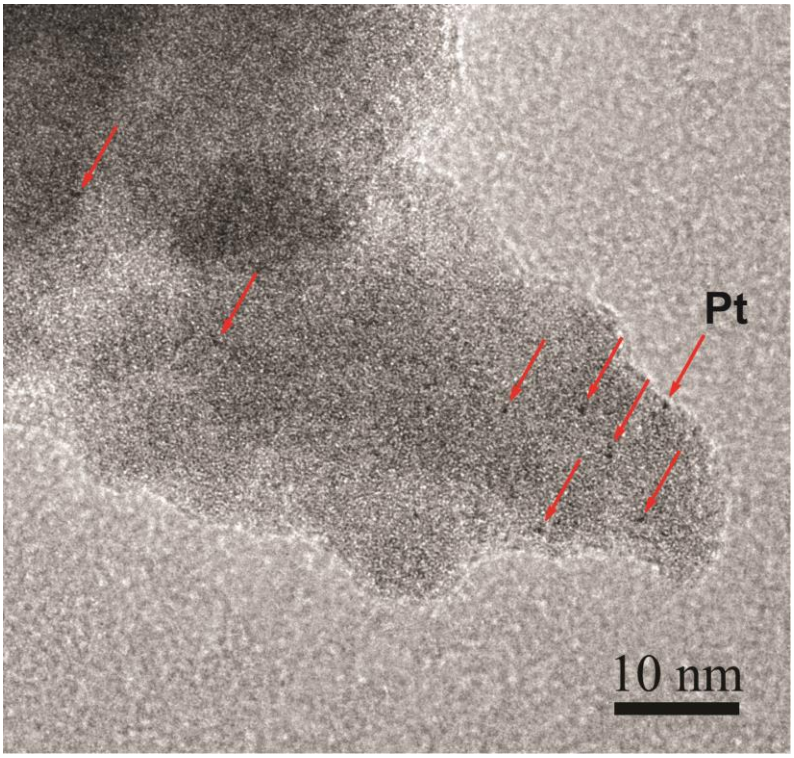

Figure S24. Bright-field TEM image of the supported Pt NPs onto the as-prepared Ta_2O_5/IL NPs (from IL **2**/water (2:2.5)). The enhanced contrast of the bright-field image suggests the presence of small Pt NPs (~1.0 nm) distributed over the Ta_2O_5 support.

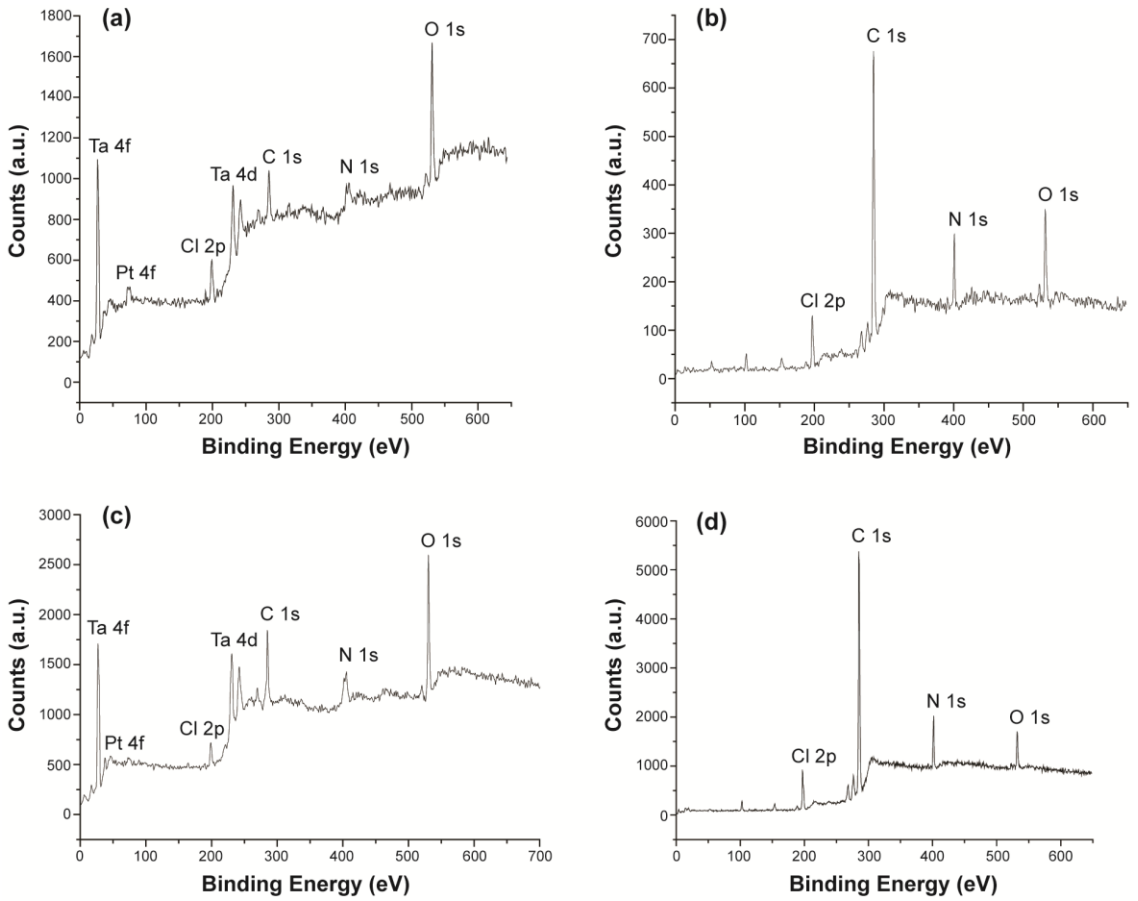

Figure S25. XPS data of the chloride ILs and Pt-supported Ta_2O_5 NPs: **(a)** Ta_2O_5/IL NPs prepared from IL **1**/water (2:2.5, IL:water initial molar ratio); **(b)** BMI.Cl; **(c)** Ta_2O_5/IL NPs prepared from IL **2**/water (2:2.5, IL:water initial molar ratio) and **(d)** DMI.Cl.

Table S3. Sample composition of Pt-supported Ta_2O_5 NPs and ILs obtained by the relative areas in the XPS analysis

	Pt-Ta_2O_5[a]	**BMI.Cl**	**Pt-Ta_2O_5[b]**	**DMI.Cl**
	(%)	**(%)**	**(%)**	**(%)**
C 1s	31.6	75.0	47.0	80.8
Ta 4f	9.4		9.2	
O 1s	32.3	8.0	27.6	3.3
N 1s	4.1	7.5	4.2	7.4
Pt 4f	2.2		1.4	
Cl 2p	20.4	9.5	10.6	8.5

[a] Ta_2O_5/IL NPs prepared from the system IL **1**/water (2:2.5); [b] Ta_2O_5/IL NPs prepared from the system IL **2**/water (2:2.5). IL/water initial molar ratio.

5. General properties of the Ta_2O_5 NPs and their activity for hydrogen production

Table S4. General properties of Ta_2O_5 NPs prepared from the hydrolysis of imidazolium tantalate ILs and their photocatalytic activity for hydrogen production

NPs (precursor)	XRD	Size (nm)	Gap (eV)	BET (m^2/g)	H_2 production ($mmol.g^{-1}.h^{-1}$)	H_2 production ($mmol.g^{-1}.h^{-1}$)[d]
Ta_2O_5/IL (IL **1**/water (2:5))[a]	Crystalline[b]	Smaller: 10 Bigger: 22	4.57	0.23	5.3	8.4
Ta_2O_5/IL (IL **1**/water (2:2.5))[a]	Crystalline[b]	3.8	4.61	0.26	3.7	5.9
Ta_2O_5/IL (IL **2**/water (2:5))[a]	Crystalline[b]	1.5	4.47	0.10	4.9	7.8
Ta_2O_5/IL (IL **2**/water (2:2.5))[a]	Crystalline[b]	6	4.64	Not determined	7.2	9.2
Ta_2O_5/after calcination (IL **1**/water (2:5))[a]	Crystalline orthorhombic	Not determined[c]	4.22	10.25	1.1	Not determined
Ta_2O_5/after calcination (IL **1**/water (2:2.5))[a]	Crystalline orthorhombic	Not determined[c]	4.15	9.36	0.9	Not determined
Ta_2O_5/after calcination (IL **2**/water (2:5))[a]	Crystalline orthorhombic	Not determined[c]	Not determined	0.20	0.8	Not determined
Ta_2O_5/after calcination (IL **2**/water (2:2.5))[a]	Crystalline orthorhombic	Not determined[c]	Not determined	3.24	0.5	Not determined

[a] IL:water initial molar ratio; [b] detected by TEM; [c] for the samples after calcination, the size of predominant large particles (bulk) were not considered; [d] in the presence of supported Pt NPs.

Table S5. Photogenerated gases from the photocatalytic reactions catalyzed by Ta_2O_5 NPs after 2.5 h

NPs (precursor)	**H_2 ($\mu mol.g^{-1}.h^{-1}$)**	**CO ($\mu mol.g^{-1}.h^{-1}$)**	**CH_4 ($\mu mol.g^{-1}.h^{-1}$)**	**CO_2 ($\mu mol.g^{-1}.h^{-1}$)**
Ta_2O_5/IL (IL **2**/water (2:2.5))	7200	0.24	0.28	0.16
Ta_2O_5/IL (IL **2**/water (2:5))	4900	0.44	0.28	0.18
Ta_2O_5/IL (IL **1**/water (2:2.5))	3700	0.44	0.22	0.16
Ta_2O_5/IL (IL **1**/water (2:5))	5300	0.44	0.36	0.16
Ta_2O_5[a] (IL **2**/water (2:2.5))	500	0.07	0.08	0.06
Ta_2O_5[a] (IL **2**/water (2:5))	840	0.06	0.10	0.06
Ta_2O_5[a] (IL **1**/water (2:2.5))	880	0.12	0.20	0.08
Ta_2O_5[a] (IL **1**/water (2:5))	1110	0.12	0.08	0.06
Ta_2O_5/IL[b] (IL **2**/water (2:2.5))	9200	0.20	1.00	0.64
Ta_2O_5/IL[b] (IL **2**/water (2:5))	7800	0.08	0.52	0.48
Ta_2O_5/IL[b] (IL **1**/water (2:2.5))	5900	0.12	0.44	0.40
Ta_2O_5/IL[b] (IL **1**/water (2:5))	8400	0.12	0.60	0.40

[a] After thermal treatment; [b] in the presence of supported Pt NPs.